Experimental Study of Low Speed Sensorless Control of PMSM Drive Using High Frequency Signal Injection

Jyoti AGRAWAL[1], Sanjay BODKHE[2]

[1]Department of Electrical Engineering, G. H. Raisoni College of Engineering, CRPF Gate No.3, Hingna Road, Digdoh Hills, Nagpur, Maharashtra - 440016, India
[2]Department of Electrical Engineering, Shri Ramdeobaba College of Engineering & Management, Ramdeo Tekdi, Gittikhadan, Katol Road, Nagpur - 440013 India

jyotigovindagrawal@gmail.com, bodkhesb@rknec.edu

Abstract. *Conventional techniques for sensorless control of permanent magnet synchronous motor drive (PMSM), which requires information on rotor position, are reviewed, and recent developments in this area are introduced in this paper along with their inherent advantages and drawbacks. The paper presents an improved method for sensorless speed control of PMSM drive with emphasis placed on signal injection method. This signal injection method examines the control performance of sensorless PMSM drive by injecting signal externally and thereby sensing the rotor position. The main objective of this drive system is to have speed control at standstill and low speed regions. Several tests are carried out to demonstrate the ability of proposed models at different operating conditions with the help of simulation results in Matlab/Simulink environment. Simulation results confirm that the proposed sensorless control approach of PMSM can achieve high performance at standstill and low speeds but not at very high speeds. An experimental setup is implemented using a 1HP surface mounted (SM) PMSM and dsPICDEM^{TM} MCHV-2 development board, to check the validity of simulation results.*

Keywords

DsPICDEM^{TM} MCHV-2 development board, high-frequency signal injection, MAT-LAB/Simulink, MPLAB X IDE, PMSM drive, sensorless, vector control.

1. Introduction

Permanent Magnet Synchronous Motor (PMSM) drives have been used widely due to its numerous advantages such as higher efficiency, higher power factor, rugged construction, reliable operation, high degree of control flexibility, high torque to inertia ratio, high torque to current ratio, etc. These advantages have attracted the interest of researchers and industry for industrial drive applications [1], [2], [3]. For the implementation of any control strategy two current sensors and knowledge of rotor position is required. In most variable speed drives an electro-magnetic resolver or optical encoder is fitted to the rotor shaft for this purpose. Though this method is precise, the presence of this shaft sensor introduces extra cost, decreases reliability and higher number of connections, thus making the total system cost very non-competitive compared to other types of motor drives. Hence, all of the above limitations make elimination of these devices very desirable [1]. From literature, it is apparent that there exist different techniques related to the sensorless control of PMSM [2]. An overview of the conventional sensorless control techniques for PMSM is presented in Fig. 1. Sensorless techniques are classified into three classes as those using the fundamental excitation models or model of the machine, those using saliency and signal injection methods and artificial intelligence methods [1]. This paper presents a performance of rotor position sensorless control of PMSM drive in which the rotor position is sensed by injecting external high frequency (HF) voltage signal in rotating q-and d-axes [4], [5]. With this scheme the difficulties in sensing the rotor position at standstill are eased. This paper tests the proposed method by various simulations and

finally some useful conclusions are drawn. The desired performance is achieved by implementing vector control technique in Matlab/Simulink and tested under different operating conditions [6]. The main aim of this drive system is to have a closed loop speed control at low speed range without using a speed transducer and the simulation results demonstrate that the proposed strategy is effective.

This paper is organized into seven sections:

- Section 1. provides a general introduction and literature review of the PMSM and a study of various existing sensorless control strategies with focus on the HF signal injection for the extraction of rotor position.

- In Section 2. , the simplified dynamic model of the PMSM is developed and is shortly examined.

- In Section 3. the signal injection technique used for extraction of rotor position is presented.

- Section 4. presents a newly developed position sensorless speed controlled PMSM drive.

- In Section 4.8. detailed simulation results under various operating conditions are presented emphasizing the merits and demerits of the method.

- Experimental setup and results are presented in Section 5. . The paper is concluded in Section 6. .
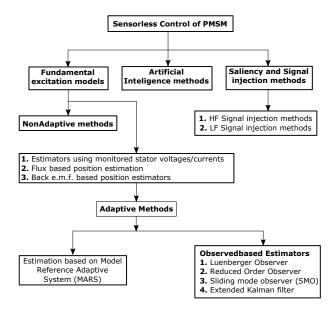
2. PMSM Model

Fig. 1: Common sensorless control techniques for PMSM.

The detailed modeling of three-phase PMSM drive system is required for proper simulation and analysis of the system. With some assumptions, the d- and q-axes stator voltages in rotor reference frame are [6]:

$$\begin{bmatrix} \nu_{ds}^r \\ \nu_{qs}^r \end{bmatrix} = \begin{bmatrix} R_S + L_d p & -\omega_r L_q \\ \omega_r L_d & R_S + L_q p \end{bmatrix} \begin{bmatrix} i_{ds}^r \\ i_{qs}^r \end{bmatrix} + \begin{bmatrix} 0 \\ \omega_r \lambda_{af} \end{bmatrix}. \tag{1}$$

From Eq. (1), it is observed that the voltage equations are equal to the product of the impedance matrix and the current vector, with an additional component due to the motionalelectro-motive force (emf) of the rotor flux linkages. The electromechanical dynamic equation is given by Eq. (2),

$$T_e = J\frac{d\omega_m}{dt} + T_1 + B\omega_m. \tag{2}$$

The dqo currents are obtained from abc currents using Park transformation as Eq. (3):

In a balanced three-phase system, the sum of three phase currents is zero. This is given by:

$$i_{as} + i_{bs} + i_{cs} = 0. \tag{4}$$

From Eq. (4), it is seen that if two currents are measured, the third-phase current can be reconstructed from the other two phase currents [7]. This eliminates the need for additional current sensors.In order to have a meaningful interpretation in the modeling, analysis and simulations, the power input to three phase machine has to be equal to the power input to two phase machine. From Eq. (1) and Eq. (2), dynamic model of PMSM in rotor reference frame is derived and is expressed by Eq. (5).

3. Implementation of Sensing Rotor Position by External HF Rotating Voltage Signal Injection

The basic scheme in signal injection is to generate a revolving voltage phasor by applying three-phase voltages at a signal frequency that is different and mostly higher than fundamental frequency [8]. This method has been used for extracting rotor position using an observer. In stationary reference frame, injected voltages at frequency ω_i are given as:

$$\begin{bmatrix} \nu_{asi} \\ \nu_{bsi} \\ \nu_{csi} \end{bmatrix} = V_i \begin{bmatrix} \sin\theta_i \\ \sin\left(\theta_i - \frac{2\pi}{3}\right) \\ \sin\left(\theta_i + \frac{2\pi}{3}\right) \end{bmatrix}, \tag{6}$$

where:

$$\theta_i = \omega_i t. \tag{7}$$

$$\begin{bmatrix} i_{qs}^r \\ i_{ds}^r \\ i_0 \end{bmatrix} = \begin{bmatrix} \cos\theta_r & \cos\left(\theta_r - \frac{2\pi}{3}\right) & \cos\left(\theta_r + \frac{2\pi}{3}\right) \\ \sin\theta_r & \sin\left(\theta_r - \frac{2\pi}{3}\right) & \sin\left(\theta_r + \frac{2\pi}{3}\right) \\ \frac{1}{2} & \frac{1}{2} & \frac{1}{2} \end{bmatrix} \cdot \begin{bmatrix} i_{as} \\ i_{bs} \\ i_{cs} \end{bmatrix}. \tag{3}$$

$$p\begin{bmatrix} i_{qs}^r \\ i_{ds}^r \\ \omega_r \\ \theta_r \end{bmatrix} = \begin{bmatrix} -\frac{R_s}{L_q} & -\frac{L_d}{L_q}\omega_r & -\frac{\lambda_{af}}{L_q} & 0 \\ \frac{L_d}{L_q}\omega_r & -\frac{R_s}{L_d} & 0 & 0 \\ \frac{\lambda_{af}}{2H} & -\frac{(L_d-L_q)i_{qs}^r}{2H} & -\frac{B}{2H} & 0 \\ 0 & 0 & 1 & 0 \end{bmatrix} \cdot \begin{bmatrix} i_{qs}^r \\ i_{ds}^r \\ \omega_r \\ \theta_r \end{bmatrix} + \begin{bmatrix} \frac{1}{L_q} & 0 & 0 \\ 0 & \frac{1}{L_d} & 0 \\ 0 & 0 & -1 \\ 0 & 0 & 0 \end{bmatrix} \cdot \begin{bmatrix} \nu_{qs}^r \\ \nu_{ds}^r \\ T_1 \end{bmatrix}. \tag{5}$$

Transforming the voltages into q- and d-axes in the same reference frame as:

$$\begin{bmatrix} \nu_{qsi} \\ \nu_{dsi} \end{bmatrix} = V_i \begin{bmatrix} \sin\theta_i \\ \cos\theta_i \end{bmatrix}. \tag{8}$$

The injected flux linkage vector in estimated rotor reference frame can be given by:

$$\begin{bmatrix} \lambda_{qsi} \\ \lambda_{dsi} \end{bmatrix} = V_{si} \sin\theta_i \begin{bmatrix} \cos\theta_{re} \\ -\sin\theta_{re} \end{bmatrix}. \tag{9}$$

The injected frequency component of the stator currents can be obtained as:

$$\begin{bmatrix} i_{qsi} \\ i_{dsi} \end{bmatrix} = \sin\theta_i \begin{bmatrix} I_1\cos\theta_{re} - I_2\cos\{2(\theta_r - \theta_{re})\} \\ -I_1\sin\theta_{re} + I_2\sin\{2(\theta_r - \theta_{re})\} \end{bmatrix}, \tag{10}$$

where:

$$I_1 = \frac{V_i}{\omega_i} \frac{\left(\frac{L_q+L_d}{2}\right)}{\left(\frac{L_q+L_d}{2}\right)^2 - \left(\frac{L_q-L_d}{2}\right)^2}, \tag{11}$$

$$I_2 = \frac{V_i}{\omega_i} \frac{\left(\frac{L_q-L_d}{2}\right)}{\left(\frac{L_q+L_d}{2}\right)^2 - \left(\frac{L_q-L_d}{2}\right)^2}. \tag{12}$$

Transforming the d-axis current to the estimated rotor position reference frames yields [9].

$$i_{dsi}^e = i_{qsi}\sin(\theta_{re}) + i_{dsi}\cos(\theta_{re}). \tag{13}$$

Equation 13 can be rewritten as:

$$i_{dsi}^e = I_2\sin\theta_i\left[\sin\{2(\theta_r - \theta_{re})\}\right]. \tag{14}$$

From Eq. 14 it can be seen that it contains the information related to rotor position error. This useful signal can be extracted using a bandpass filter (BPF) which separates the fundamental component from the HF component followed by an observer. This position error can be demodulated by any demodulation schemebut in this model heterodyning process is usedfor the estimation of position and speed [5].

4. Implementation of Speed-Controlled Sensorless PMSM Drive by Estimating Rotor Position Using Signal Injection

The proposed model developed for sensorless vector control of PMSM drive using signal injection, as presented in Fig. 2, is implemented using the software Matlab/Simulink. It consists of a speed loop, current and torque angle calculator, stator current synthesizer, inverter with SPWM current control, PMSM model, HF signal injection, demodulation process, controller and observer for rotor position and speed estimation. Each functional block is elaborated in detail in the following sections. The principle for this speed control strategy is based on comparing the reference speed and the estimated speed [10]. The speed error thus obtained is then processed through the speed controller and the output of this block represents the reference torque (T_e^*) for the current and torque angle calculator. The stator current synthesizer generates the phase reference current commands. The three phase reference currents are compared with their respective actual currents resulting in the current errors in a PWM current controller which is then used to generate the switching signals for the inverter. In the proposed scheme the feedback signal i.e. rotor position (θ_{re}) is estimated using external signal injection scheme. Once the rotor position is estimated, the rotor speed (ω_{re}) can be estimated by using Eq. (6) [11]. The inability with most of the methods to provide accurate rotor position estimation at low speeds, which directly affects the control performance, would not be a problem with this technique [12].

4.1. Speed Controller

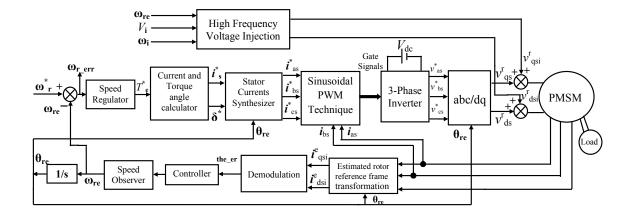The speed error between command and estimated values of speed is processed in the proportional and inte-

Fig. 2: Overall schematic of the sensorless vector control for a speed controlled PMSM drive by using external high frequency signal injection scheme.

gral (PI) speed controller to generate a reference torque [10]. The main aim of the speed controller is to control the electromagnetic torque so that the speed error can be minimized.

4.2. Electromagnetic Torque

The expression for the electromagnetic torque (T_e) developed on the rotor can be obtained from the input power and its various components as given by Eq. (15) [13].

$$T_e = \frac{3}{2}\frac{P}{2}\left[(L_d - L_q)\, i_{ds}^r + \lambda_{af}\right] i_{qs}^r. \qquad (15)$$

4.3. SPWM Current Controlled Inverter Model

Figure 2 shows that the PMSM is fed from a voltage source inverter with current control. The switching frequency is usually fixed at carrier frequency (f_c). The switching signals for the power devices are determined by the intersection of a triangular carrier wave of desired switching frequency with error of the controlled signal obtained from the reference and actual phase currents. The comparison will result in a signal that will demand the phase voltage to follow in such a way that the current error of the respective phase is reduced to zero [14].

4.4. The d- and q-axes Stator Current in Rotor Reference Frame

By using Eq. (5), the d and q-axis model is constructed which is shown in Fig. 3.

4.5. Creation of HF Revolving Voltage Vector Injection

A balanced set of three phase voltage vector given in Eq. (6) with low amplitude (V_i) and high frequency fi- are transformed into d- and q-axes by using Eq. (8). These voltages are transformed into the estimated position reference frames (refer Fig. 4) and then added to the controlled dq output voltages.

4.6. Demodulation Process

Figure 5 consists of BPF which aims at separating the injected signal from the fundamental component. In order to extract rotor position error needed for the observerthe BP filteredsignal i.e. Eq. (15) is demodulated and then multiplied by $e^{-j(\omega it)}$ [15]. This signal is then cleaned by a low-pass filter which removes the second harmonic component leaving the desired error term only. The rotor position thus can be estimated from this signal using an observer [16]. Simulink model developed for this purpose is shown in Fig. 5.

4.7. Controller and Observer

In order to extract rotor position and speed from the position error a tracking observer is required. The internal structure of the controller is developed in
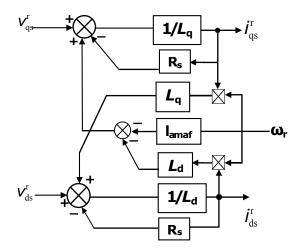
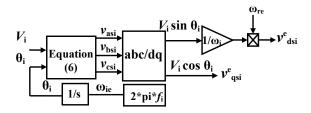**Fig. 3:** Dynamic model of PMSM in rotor reference frame.

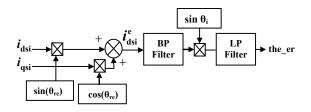**Fig. 4:** Common Revolving voltage injection scheme PMSM.

Fig. 5: Implementation of demodulation process.

Simulink to perform this function (see Fig. 6. The detected rotor position error can be used for estimating the rotor position and speed [2]. Once the rotor speed is estimated accurately, the rotor position can be obtained by using an integrator. The electromagnetic torque signal is added at the output of controller for faster dynamics [2].

4.8. Simulation Results and Discussion

A sensorless speed-controlled PMSM drive has been developed in MATLAB environment to validate the proposed speed and position estimation method. The functionality of the implemented sensorless control method is verified by testing the drive under different

operating conditions. The plots of speed, torque, currents, rotor position and position error are given. The plotted variables are in normalized units (p.u.). The test results of the sensorless controlled PMSM drive employing HF signal injection scheme for five different operating conditions are shown in Fig. 7, Fig. 8, Fig. 9, Fig. 10. The parameters for PMSM used in the simulation are given in the appendix. Sampling time is set to $1e^{-6}$ s. The rated speed of $628.6 \text{ rad·}s^{-1}$ is selected as base speed. The injected frequency (f_i) is 2 kHz and the amplitude (V_i) is 10 V. In order to verify the accuracy of proposed estimated method and also to study the response of position sensorless drive under different dynamic conditions it is important to compare the two different methods. In the first method the rotor speed and position are estimated using the proposed model as described in Fig. 2 while in the second method, the same machine variables i.e. rotor speed and position are calculated using the dynamic model of PMSM which is treated as actual model.

4.9. Free Acceleration Characteristics

In this test, the motor drive is allowed to accelerate from $0 \text{ rad·}s^{-1}$ to rated speed i.e. $628.6 \text{ rad·}s^{-1}$ (1 p.u.) considering 10 % of the rated load. From Fig. 7(a), it is concluded that though the estimated rotor speed matches the reference speed nearly at 0.09 s. The simulation resultsincluding a comparison of the actual and estimated rotor angle are shown in Fig. 7(d), while the position error is plotted underneath it. As observed from the Fig. 7(e), there is no appreciable deviation in rotor position trackingas long as the rotor speed is not very high, till the correct rotor position is detected i.e. after about 0.09 s.
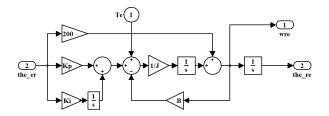

Fig. 6: Simulink model of rotor position and speed estimatorusing rotor position error tracking observer.

4.10. Low Speed and Standstill Operation

One of the biggest challenges in sensorless vector control of PMSM is estimating rotor position at low speed including standstill in which most of the methods fail. In this test the speed control performance at low speed including standstill under no load condition is shown
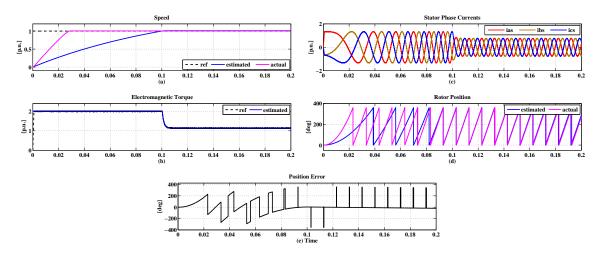
Fig. 7: Free acceleration characterisitc: (a) Reference, estimated and actual rotor speed response, (b) Torque response, (c) Stator phasecurrents response, (d) Estimated and actual rotor position, (e) Rotor position error ($\delta\theta$).
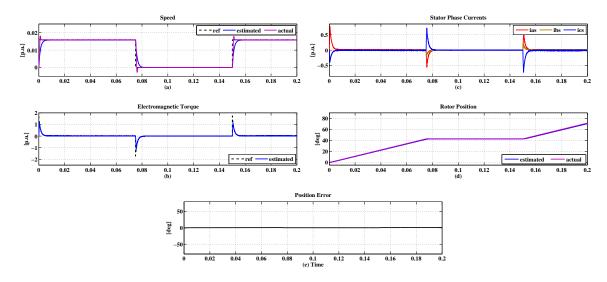

Fig. 8: Step change in reference speed from 10 rad·s^{-1} to 0 rad·s^{-1} at 0.075 s and back to 10 rad·s^{-1} at 0.015 s under no load: (a) Reference, estimated and actual rotor speed response, (b) Torque response, (c) Stator phase currents response, (d) Estimated and actual rotor position, (e) Position error ($\delta\theta$).

in Fig. 8(a). The speed command is varied from 10 rad· s^{-1} to 0 rad· s^{-1} at 0.075 s and back to 10 rad· s^{-1} at 0.15 s in step manner as it is represented in Fig. 8(a). The rotor speed is accelerated from standstill to 10 rad· s^{-1} starting from $t = 0$ s so that the motor successfully runs at the reference speed. Figure 8(c) presents that the stator phase currents response and Fig. 8(b) presents the torque response which is just sufficient to overcome friction except at transitions of the sharp speed variations (see Fig. 8(a)) [17], [18].

4.11. Step Change in Reference Speed

Figure 9 shows the simulation result for speed control with a step change in reference speed at rated load. At 0.05 s, the reference speed is step changed from

50 rad· s^{-1} to 150 rad·s^{-1}, then 200 rad·s^{-1} at 0.1 s and finally set to 250 rad· s^{-1} at 0.15 s. As observed from the Fig. 9(d) the estimated rotor position waveform follows the actual rotor position. Figure 9(e) shows the waveform of error in rotor position i.e. the difference between the estimated and actual rotor position ($\delta\theta = \delta_r - \theta_{re}$). From the plot of rotor position error it is seen that the error is driven to zero which indicates how well the position estimation scheme

4.12. Speed Reversal Operation

In this test, the motor drive covers both the direction of rotation. The speed reference is step changed from 375 rad·s^{-1} to -375 rad·s^{-1} at 0.1 s. From Fig. 10(a) and Fig. 10(b) it is seen that with a positive speed command the electromagnetic torque is driven to pos-

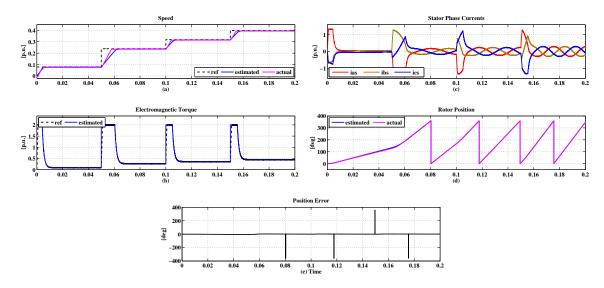**Fig. 9:** Step change in reference speed from 10 rad·s^{-1} to 0 rad·s^{-1} at 0.075 s and back to 10 rad·s^{-1} at 0.015 s under no load: (a) Reference, estimated and actual rotor speed response, (b) Torque response, (c) Stator phase currents response, (d) Estimated and actual rotor position, (e) Position error ($\delta\theta$).
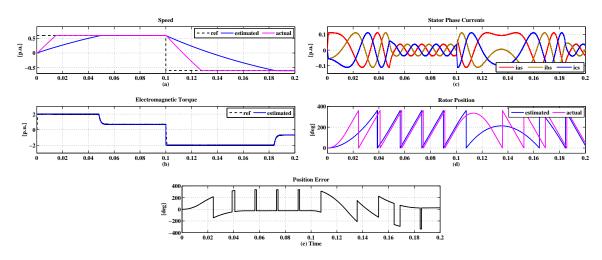

Fig. 10: speed changes from 375 rad·s^{-1} to -375 rad·s^{-1} at 0.1 s under no load: (a) Reference, estimated and actual speed, (b) Torque, (c) Stator currents, (d) Estimated and actual position, (e) Position error ($\delta\theta$).

itive maximum and is maintained there until actual speed matches the reference speed (ω_r^*) [15]. When the estimated speed matches the reference speed, the torque comes down to match the load torque and the friction torque [19]. With a negative speed command the electromagnetic torque is driven to negative maximum, which causes the reverse rotation. The speed error causes ripples which are not even noticeable (see Fig. 10(c)) [19].

5. Experimental Setup and Results

To support the simulation results, the complete proposed scheme is implemented and tested using a dsPIC-

DEM MCHV-2 development board manufactured by Microchip Technology Inc. The carrier frequency of the high speed PWM module is set to 20 kHz. The three-phase bridge inverter with a power rating of 400 V / 6.5 A has six sets of IGBTs. The real test bench employed for sensorless control of PMSM is presented in Fig 11. The proposed algorithm for speed estimation is developed using MPLAB X IDE. The test motor is a Y-connected, 1 HP, 4.5 Amp, 4000 rpm SMPMSM with detailed parameters enumerated in Table (1). PMSM is equipped with built-in position encoder used only for monitoring the estimated speed not for speed control.

Tab. 1: Rating and Parameters of a 1HP PMSM.

Rating		
Symbol	**Quantity**	**Value and units**
N	Rated speed	4000 rpm
f	Rated frequency	50 Hz
V_{L-L}	Rated line-line rms voltage	240 V
I_{RMS}	Rated rms current	4 A
T_L	Rated torque	6 N-m
Parameters		
Symbol	**Quantity**	**Value and units**
P	Pole pairs	3
L_s	Stator winding inductance	0.005129 (H)
R_s	Stator winding resistance	3.0832 (Ω)
K_E	Back-EMF constant	52.6 ($\text{V}_{pk}\cdot\text{kRPM}^{-1}$)
λ_{pm}	Permanent magnet flux-linkage	0.1887 (Wb)
K_t	Torque constant	0.8554 ($\text{Nm}\cdot\text{A}^{-1}$)
T_{max}	Peak torque	6 N-m
PPR	Quadrature encoder	2048 PPR

5.1. Step Change in Reference Speed

Figure 12, Fig. 13, Fig. 14 and Fig. 15 shows the experimental results for sensorless speed control of PMSM with a step change in reference speed command (refer Fig. 12)under no load condition. At 14 ms, the reference speed is step changed from 2000 rpm to 3000 rpm, then from 3000 rpm to 2500 rpm at 47 ms and finally set to 2000 rpm at 119 ms. As observed from the Fig. 14 the estimated rotor position waveform tracks the actual rotor position shown in Fig. 13 very nicely. It is also clear from the waveform of rotor speed error as shown in Fig. 15, how well the proposed scheme handles this type of reference speed command.
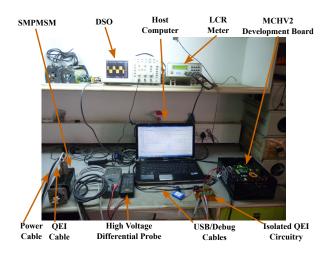

Fig. 11: Photograph of experimental test bench.
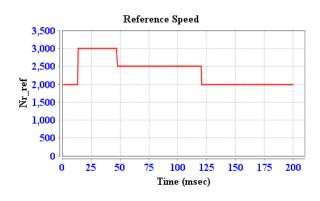

Fig. 12: Reference speed changes from 2000 rpm to 3000 rpm at 14 ms, then to 2500 rpm at 47 ms and finally back to 2000 rpm at 119 ms under no load (Reference speed).
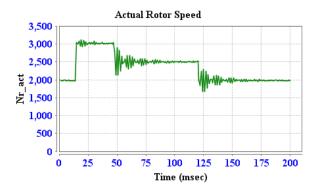

Fig. 13: Reference speed changes from 2000 rpm to 3000 rpm at 14 ms, then to 2500 rpm at 47 ms and finally back to 2000 rpm at 119 ms under no load (Actual rotor speed).
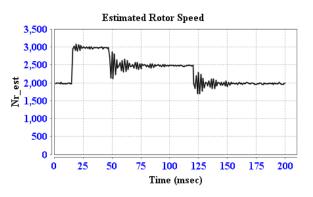

Fig. 14: Reference speed changes from 2000 rpm to 3000 rpm at 14 ms, then to 2500 rpm at 47 ms and finally back to 2000 rpm at 119 ms under no load (Estimated rotor speed).

5.2. Low Speed Operation

Figure 16, Fig. 17, Fig. 18, Fig. 19 shows the experimentalresults for reference speed command of 400 rpm under no load. From the waveform of rotor speed error presented in Fig. 18, it is observed that there is an error of approximately 20 rpm.
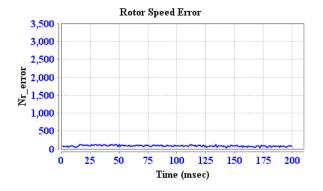
Fig. 15: Reference speed changes from 2000 rpm to 3000 rpm at 14 ms, then to 2500 rpm at 47 ms and finally back to 2000 rpm at 119 ms under no load (Rotor speed error).

Fig. 16: Low speed operation for reference speed of 400 rpm under no load (Actual rotor speed).
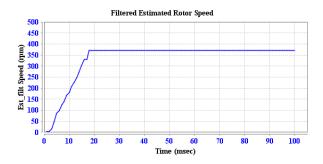

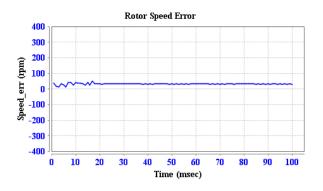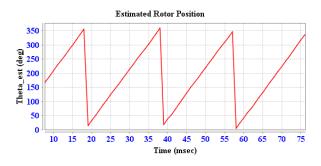**Fig. 17:** Low speed operation for reference speed of 400 rpm under no load (Estimated rotor speed).

Fig. 18: Low speed operation for reference speed of 400 rpm under no load (Rotor speed error).

Fig. 19: Low speed operation for reference speed of 400 rpm under no load (Estimated rotor position).

6.   Conclusions

The mathematical modeling for analysis of sensorless vector controlled PMSM drive and its implementation employing HF signal injection using MATLAB/Simulink has been presented in this paper. It is concluded from the literature that many sensorless scheme cannot be used at low and zero speed where back EMF signal is not available.To achieve operation at such speed the signal injection scheme can be more efficient than any other sensorless method. Finally it can be concluded from the simulation and experimental results that the signal injection strategy appears to be good at low speed and standstill but it cannot give good performance at high and very high speed. Performance of sensorless PMSM is investigated under various operating conditions to verify the validity and feasibility of the proposed model.It must be noted that the HF signal injection method can beextended to a wide speed range but not by increasing the injection frequency as it may start overlapping with the inverter's switching frequency. But the problem faced by this scheme is, it requires observer for successful operation. Furthermore, HF signal injection technique is robust to parameter variations.

References

[1] VAS, P. *Sensorless Vector and Direct Torque Control.* 1st. ed. Oxford: Oxford University Press, 1998. ISBN 978-0-1985-6465-2.

[2] KRISHNAN, R. *Permanent Magnet Synchronous and Brushless DC Motor Drives.* 1st. ed. Florida: CRC Press, 2010. ISBN 978-0-8247-5384-9.

[3] BOLDEA, I. and S. A. NASAR. *Electric Drives.* 2nd. ed. Florida: CRC Press, 2006. ISBN 978-0-8493-4220-2.

[4] TOUDERT, O. M., H. ZEROUG, F. AUGER and A. CHIBAH. Improved rotor position estimation of salient-pole PMSM using high frequency carrier signal injection. In: *IEEE International Conference on Mechatronics.* Vicenza: IEEE, 2013, pp. 761–767. ISBN 978-1-4673-1386-5. DOI: 10.1109/ICMECH.2013.6519137.

[5] CORLEY, M. J. and R. D. LORENZ. Rotor position and velocity estimation for a slient-pole permanent magnet synchronous machine at standstill and high speeds. *IEEE Transactions on Industry Applications.* 1998, vol. 34, iss. 4, pp. 784–789. ISSN 0093-9994. DOI: 10.1109/28.703973.

[6] PILLAY, P. and R. KRISHNAN. Modeling, simulation, and analysis of permanent-magnet motor drives, Part I: The permanent-magnet synchronous motor drive. *IEEE Transactions on Industry Applications.* 1989, vol. 25, iss. 2, pp. 265–273. ISSN 0093-9994. DOI: 10.1109/28.25541.

[7] MISHRA, A., J. A. MAKWANA, P. AGARWAL and S. P. SRIVASTAVA. Modeling and implementation of vector control for PM synchronous motor drive. In: *International Conference on Advances in Engineering, Science and Management (ICAESM).* Nagapattinam: IEEE, 2012, pp. 582–585. ISBN 978-1-4673-0213-5.

[8] CHEN, Z., X. DENG, K. HUANG, W. ZHEN and L. WANG. Sensorless control of wound rotor synchronous machines based on high-frequency signal injection into the stator windings. *Journal of Power Electronics.* 2013, vol. 13, iss. 4, pp. 669–678. ISSN 1598-2092. DOI: 10.6113/JPE.2013.13.4.669.

[9] LI, Y., Y. ZHANG and T. ZHANG. Simulation and experimental studies of speed sensorless control of permanent magnet synchronous motors for mini electric locomotive drive. *Journal of Control and Automation.* 2014, vol. 7, iss. 2, pp. 55–68. ISSN 2005-4297. DOI: 10.14257/ijca.2014.7.1.05.

[10] KRISHNAN, R. *Electric Motor Drives: Modeling, Analysis, and Control.* 1st. ed., Upper Saddle River: Prentice-Hall, 2001. ISBN 978-0-1309-1014-1.

[11] PILLAY, P. and R. KRISHNAN. Control characteristics and speed controller design for a high performance of permanent magnet synchronous motor drive. *IEEE Transactions on Power Electronics.* 1990, vol. 5, iss. 2, pp. 151–159. ISSN 0885-8993. DOI: 10.1109/63.53152.

[12] MISHRA, A., J. A. MAKWANA, P. AGARWAL and S. P. SRIVASTAVA. MRAS based estimation of speed in sensorless PMSM drive. In: *IEEE Fifth Power India Conference.* Murthal: IEEE, 2012, pp. 1–5. ISBN 978-1-4673-0763-5. DOI: 10.1109/PowerI.2012.6479492.

[13] PILLAY, P. and R. KRISHNAN. Modeling of permanent magnet motor drives. *IEEE Transactions on Industrial Electronics.* 1988, vol. 35, iss. 4, pp. 537–541. ISSN 0278-0046. DOI: 10.1109/41.9176.

[14] WOOD, P. *Theory of Switching Power Converter.* 1st. ed. New York: Van Nostrand-Reinhold, 1981.

[15] ISHAK, A. D., S. IQBAL and M. KAMAROL. A speed sensorless field oriented control of parallel- connected dual PMSM. In: *IEEE International Conference on Control System, Computing and Engineering (ICCSCE).* Penang: IEEE, 2011, pp. 567–570. ISBN 978-1-4577-1640-9. DOI: 10.1109/ICCSCE.2011.6190590.

[16] SUL, S. K. *Control of Electric Machine Drive Systems.* 1st. ed. Wiley-IEEE Press, 2011. ISBN 978-0-4705-9079-9.

[17] HOLTZ, J. Acquisition of position error and magnet polarity for sensorless control of PM synchronous machines. *IEEE Transactions on Industry Applications.* 2008, vol. 44, iss. 4, pp. 1172–1180. ISSN 0093-9994. DOI: 10.1109/TIA.2008.921418.

[18] ZHAO, Y., W. QIAO and L. WU. Compensation algorithms for sliding mode observers in sensorless control of IPMSMs. In: *IEEE International Electric Vehicle Conference (IEVC).* Greenville: IEEE, 2012, pp. 1–7. ISBN 978-1-4673-1562-3. DOI: 10.1109/IEVC.2012.6183241.

[19] BRANDSTETTER, P. and T. KRECEK. Estimation of PMSM magnetic saliency using injection technique. *Journal Electronics and Electrical Engineering.* 2014, vol. 20, iss. 2, pp. 22–27. ISSN 9442-6310. DOI: 10.5755/j01.eee.20.2.4784.

About Authors

Jyoti AGRAWAL received the M.Tech degree and is currently pursuing the Ph.D. degree both in electrical engineering from GHRCE, Nagpur, India. Her research interests include electric motor drives and power electronics.

Sanjay BODKHE received the Ph.D. degree in electrical engineering from VNIT, Nagpur, in 2011. His research interests are electric motor drives, power electronics and smart grid.